Science Advances
AAAS

advances.sciencemag.org/cgi/content/full/7/10/eabe2866/DC1

Supplementary Materials for

Spontaneous phase segregation of Sr_2NiO_3 and $SrNi_2O_3$ during $SrNiO_3$ heteroepitaxy

Le Wang, Zhenzhong Yang, Xinmao Yin, Sandra D. Taylor, Xu He, Chi Sin Tang, Mark E. Bowden, Jiali Zhao, Jiaou Wang, Jishan Liu, Daniel E. Perea, Linda Wangoh, Andrew T. S. Wee, Hua Zhou, Scott A. Chambers*, Yingge Du*

*Corresponding author. Email: sa.chambers@pnnl.gov (S.A.C.); yingge.du@pnnl.gov (Y.D.)

Published 5 March 2021, *Sci. Adv.* **7**, eabe2866 (2021)
DOI: 10.1126/sciadv.abe2866

This PDF file includes:

Figs. S1 to S5

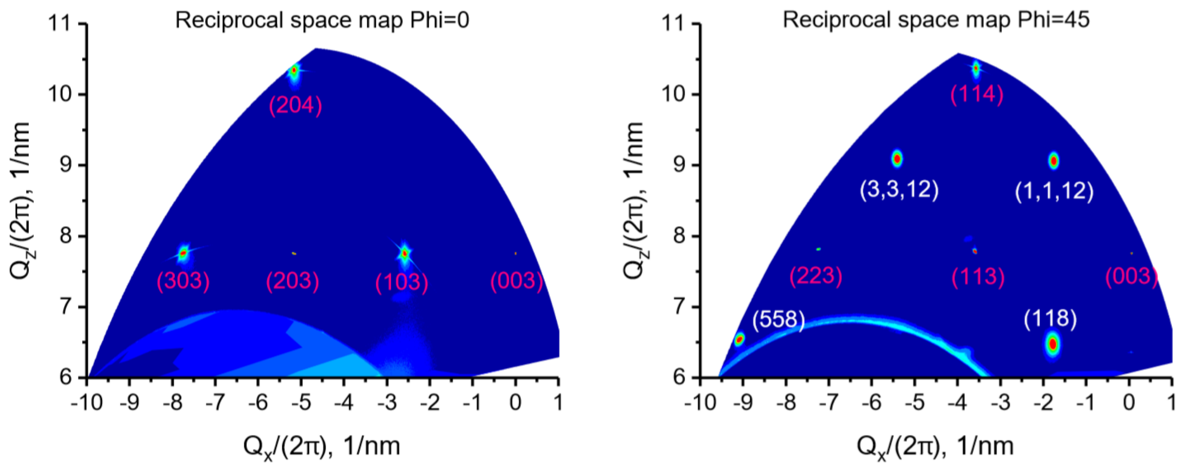

Figure S1. Wide-range RSM for 25 nm SNO/LSAT(001) measured along phi = 0° and phi = 45°, where x corresponds to the [100] direction (left) and [110] direction (right) of the LSAT substrate, z corresponds to the [001] direction. The film and substrate peak indices are written in white and purple, respectively.

When scanning the sample along 0°, we did not observe any film peaks, indicating a lack of coherent (0kl) planes extending for sufficient length. However, when we scan it along 45°, the film peaks appear exactly half-way between the substrate peaks in the x direction, indicating that the film is coherently strained to the substrate along this direction.

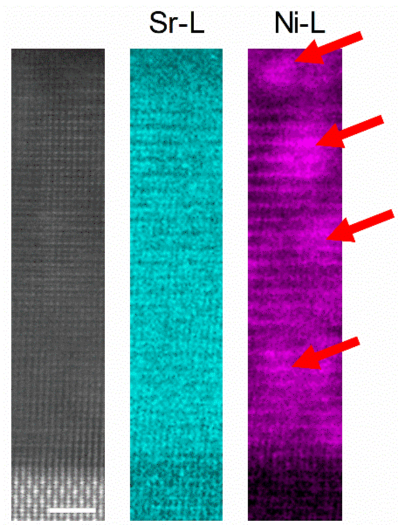

Figure S2. HAADF STEM image (left, scale bar is 2 nm) and corresponding individual EELS maps (right) for the Sr $L_{2,3}$, and Ni $L_{2,3}$ ionization edges at lower magnification. The red arrows show some NiO clusters existed in the SNO films.

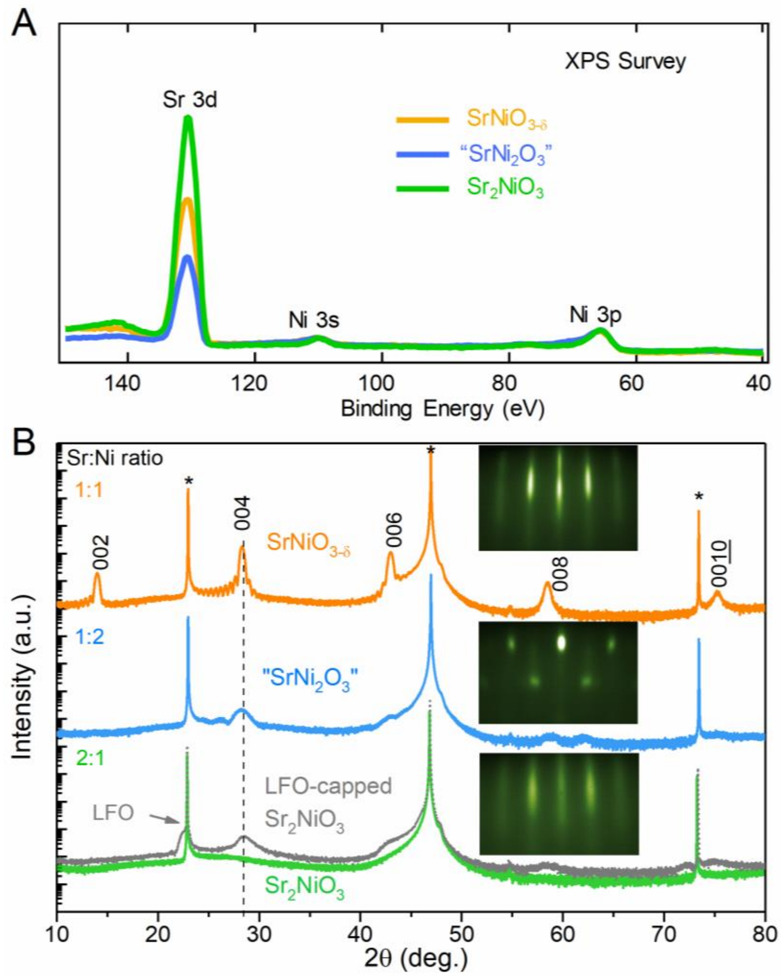

Figure S3. XPS survey scans and XRD θ-2θ scans of SNO films with different Sr/Ni ratios. (**A**) XPS survey scans of SNO films with different Sr/Ni ratios. All Ni 3*p* spectra were normalized. The intensities of the Sr 3*d* spectra show the distinct differences and are consistent with the targeted Sr:Ni flux ratios. (**B**) XRD θ-2θ scans of SNO films with different Sr/Ni ratios. The stars denote the diffraction peaks from LSAT substrates. The insets show the corresponding RHEED patterns for the as-grown SNO films on LSAT(001) viewed along the [100] zone axis. The SNO film with a Sr/Ni ratio of 2:1 was found to become amorphous once exposed in ambient atmosphere, consistent with the previous study.(21) XRD θ-2θ scan of one $LaFeO_3$ (LFO)-capped Sr_2NiO_3 sample was also included for comparison. The thickness of the capping layer is ~10 nm. The black dashed line denotes the same peak position for these three samples, indicating the same *c*-axis lattice parameter.

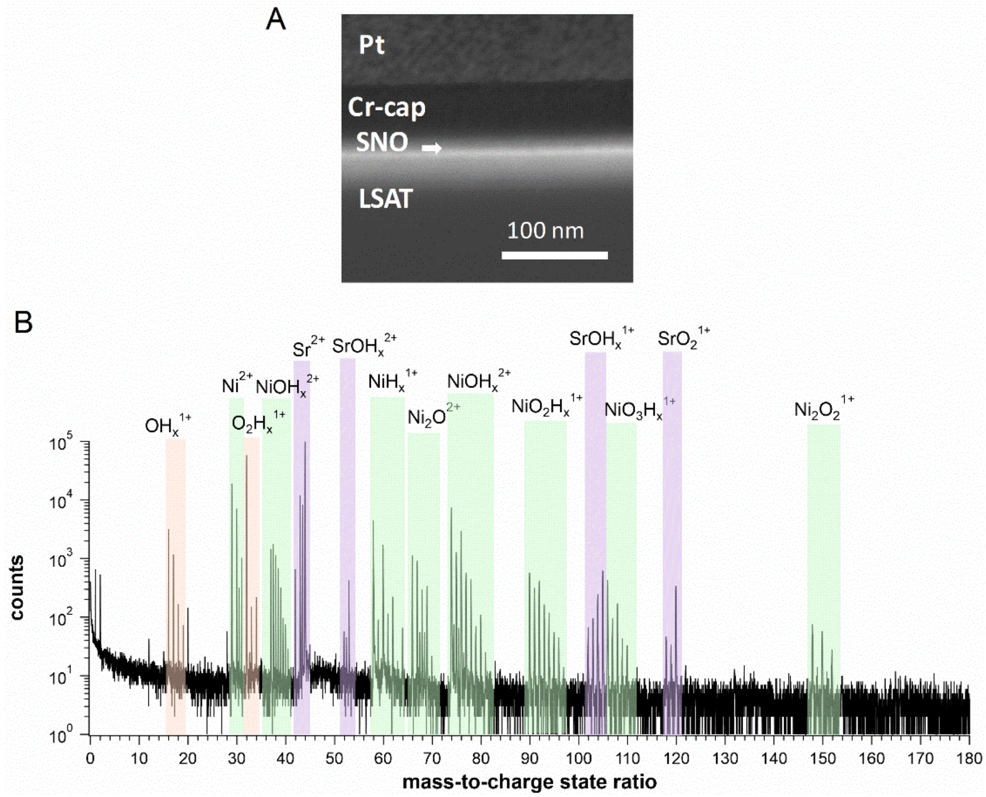

Figure S4. Cross-sectional view of SNO/LSAT sample in SEM and Mass spectrum. (**A**) Cross-sectional view of SNO/LSAT sample in Scanning electron microscope (SEM). (**B**) Mass spectrum of SNO films from atom probe tomography (APT) highlighting the assignment of ionic species.

The surface of SNO/LSAT was coated with ~50 nm Cr and prepared into APT tips using conventional focused-ion beam milling techniques in a dual-beam scanning electron microscope (FEI Helios Nanolab). Protective Pt capping layers were deposited on a rectangular section of the surface (e.g., ~2 µm × 15 µm) by ion-beam induced deposition using the dual-beam FIB microscope, further protecting the Cr/SNO interface from damage and Ga contamination during ion milling. A lamellar wedge was created by trench milling on both sides with the ion beam (Ga+ ion, 30 kV) and was extracted with the Omniprobe micromanipulator. Sections of the wedge were mounted over several Si microposts, making several APT tips (i.e., five tips). Each section was annular milled to obtain needle-shaped APT specimens with <100 nm tip diameter. The tip configuration and sequence of phases includes ~50 nm Cr, ~20 nm SNO, and the LSAT substrate horizontally stacked on top of one another. The tips were intentionally milled such that the topmost layer included Cr to protect and capture the SNO film, the region of interest in this study.

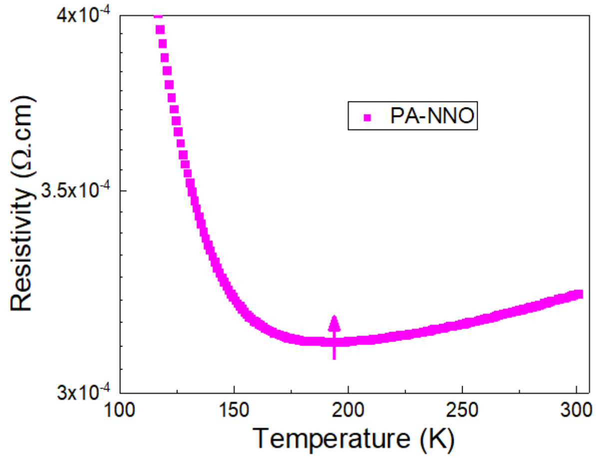

Figure S5. Temperature dependent resistivity of PA-NNO. The purple arrow denotes the metal-insulator transition point (T_{MI}).